

3-4 Development and Stable Operation of Femtosecond Laser Frequency Combs toward Optical Frequency Standards

NAGANO Shigeo, ITO Hiroyuki, LI Ying, KUMAGAI Motohiro, Clayton R. Locke, John G. Hartnett, and HOSOKAWA Mizuhiko

Optical frequency standards are being developed worldwide to lead a new definition of the unit of time. An optical frequency comb based on a femtosecond-pulse mode-locked laser is a key component for the development of optical frequency standards, since it enabled to directly link the optical and microwave frequencies with unprecedented accuracy. We have developed femtosecond-laser optical frequency combs and applied them to the absolute frequency measurements of a clock laser for optical frequency standards in NICT. In this article, we present the characteristics of the optical frequency combs developed.

Keywords

Optical frequency standard, Optical clock, Optical frequency comb, Femtosecond-pulse mode-locked laser

1 Introduction

Atomic frequency standards based on the quantum transition in the optical region are being developed worldwide. The optical frequency standards are confidently expected to lead a new definition of the unit of time, since they have intrinsically higher accuracy and stability than the microwave atomic clocks based on the hyperfine transition in cesium. Such optical standards are needed not only for realization of accurate clocks and time scale but expansion of our knowledge regarding fundamental physics by the measurement of frequencies related to the numerous physical quantities[1]-[3].

The development of optical frequency standards has been implemented in many research laboratories and universities. However, the large frequency difference between the optical standard and present standard in microwave region by more than five orders of magnitude had prevented to compare their frequencies. The

microwave-optical frequency chains were employed to compare the frequencies in spite of complicated devices requiring significant resources for operation[4]. It was also difficult to connect the microwave standard to the optical one without the degradation of the measurement accuracy. An optical frequency comb generated from the femtosecond (fs)-pulse mode-locked laser, which was invented at the end of the last century, revolutionized the precise frequency metrology in optical region and enabled us to directly connect the optical to microwave frequency with high accuracy[5][6]. The femtosecond laser frequency comb (FLFC) drastically improved the measurement accuracy of the optical frequency, and it has opened a new possibility for realization of the optical frequency standards.

The fundamental configuration of most of those optical frequency standards is a narrow-linewidth clock laser stabilized to a resonance frequency of microscopic quantum systems,

with a clockwork device for the counting and display. The clock laser is pre-stabilized to a Fabry-Perot (FP) optical cavity to narrow its linewidth and improve the short-term stability. The state-of-the-art quantum system may be classified into a single ion trapped by suitable electric field and ensemble of neutral atoms confined in the potential wells of an optical lattice. Their atomic transitions are well-isolated from environment, and serve as the best absolute frequency references. Thus, the clock laser obtains the long-term stability as well as the short-term one by steering its frequency to the atomic resonance. The laser frequency is counted by a FLFC linked to the microwave standard and accumulated a defined number of the cycle to register the second of time. The output of the FLFC is also applicable to establish a new frequency standard in optical and/or microwave region.

2 Femtosecond-pulse mode-locked laser optical frequency comb

2.1 Principle of femtosecond laser frequency combs

A fs-pulse mode-locked laser has a potential to be an optical frequency counter. It is based that the multiple longitudinal modes emitted from the mode-locked laser, so-called optical frequency comb, are available as a precise ruler in optical frequency. The mode-locked laser generates the repetitive pulse as shown in Fig. 1(a). To calculate the effect of a pulse-to-pulse phase shift on the spectrum, the electric field amplitude of the single pulse is written by is $E_1(t) = \hat{E}(t - m\tau_r)\exp(i\omega_c t + i\phi_0)$. Then, the electric field of the pulse train at a fixed spatial location is

$$E(t) = \sum_m \hat{E}(t - m\tau_r) e^{i\{\omega_c t - m\omega_c \tau_r + m\Delta\phi + \phi_0\}} \quad (1)$$

where \hat{E} is the pulse envelop, ω_c is the carrier angler frequency, ϕ_0 is the overall phase offset and τ_r is the time between pulses[7]. $\Delta\phi$ is called carrier-envelope (CE) offset phase and repre-

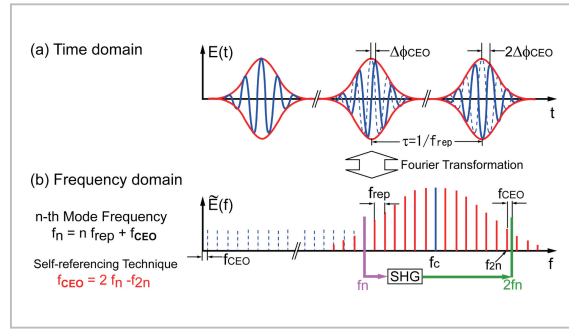


Fig.1 Principle of femtosecond laser optical frequency combs

The output field of a mode-locked laser in the time domain (a) and frequency domain (b). The concept of the self-referencing technique for the measurement of the carrier-envelope offset frequency f_{ceo} is also illustrated in the frequency domain.

sents the phase between the carrier and the envelope, which evolves from pulse to pulse. The Fourier transform of $E(t)$ is calculated to be

$$E(\omega) = e^{i\phi_0} \sum_m e^{i\{m\Delta\phi - m\omega\tau_r\}} \tilde{E}(\omega - \omega_c) \quad (2)$$

where $\tilde{E}(\omega) \equiv \int dt \hat{E}(t) \exp(-i\omega t)$. The significant components in the spectrum are the ones for which the exponential in the sum add coherently because the phase shift between the pulse n and $n+1$ is a multiple of 2π . This yields a comb spectrum with angler frequencies $\omega = 2n\pi/\tau_r + \Delta\phi/\tau_r$, where n is an integer. It is converted to

$$f(n) = nf_{rep} + f_{ceo} \quad (n : \text{a large integer}) \quad (3)$$

from the angular frequency, where the pulse repetition frequency as $f_{rep} \equiv 1/\tau_r$ and the CE offset frequency as $f_{ceo} \equiv (\Delta\phi/2\pi) f_{rep}$. The spectral components of the pulse train emitted by the mode-locked laser, which form the optical comb as shown in Fig. 1(b), are spaced by f_{rep} and shifted by f_{ceo} in the Fourier frequency domain. In other word, the frequency of n -th component $f(n)$ of the FLFC is entirely determined by the two frequencies.

The measurement of the laser frequency

is performed by heterodyning a laser oscillating at a single frequency against nearby n -th component of the FLFC. The heterodyne radio-frequency (rf) signal contains beat at frequency $f_{\text{beat}} = f_{\text{cw}} - nf_{\text{rep}} - f_{\text{ceo}}$, when the continuous-wave (cw) laser frequency f_{cw} is assumed to be higher than $f(n)$. It should be noted that f_{beat} , f_{rep} , and f_{ceo} are accessible and can be measured with ordinary rf equipments. There remains arbitrariness with signs of f_{beat} and f_{ceo} and determination of n . They will be discussed later. For the precise frequency measurement, both f_{rep} and f_{ceo} must be locked on the microwave standard.

The signal extraction for controlling f_{rep} and f_{ceo} is essential for the frequency metrology. f_{rep} can be measured by monitoring the pulse train. A fast photodiode is used to directly detect a fraction of the output power of the mode-locked laser. Contrary to the detection of f_{rep} , the measurement of f_{ceo} is required a more challenging manner. The self-referencing technique is often employed to observe f_{ceo} without an auxiliary laser oscillating at a calibrated frequency[5]. As illustrated in Fig. 1(b), the technique can extract f_{ceo} as a beatnote by comparing the long-wavelength portion of the octave-spanning spectrum (around n -th mode) after frequency doubling to the short-wavelength one (around $2n$ -th mode). This beatnote measurement can be describes as following equation:

$$2f(n) - f(2n) = 2(nf_{\text{rep}} + f_{\text{ceo}}) - (2nf_{\text{rep}} + f_{\text{ceo}}) = f_{\text{ceo}} \quad (4)$$

The fact that many comb lines contribute to the beatnote signal means that a strong signal can be obtained even if the one-mode light power produced by the second-harmonic generation (SHG) is weak.

The broad spectrum over an octave is essential for the self-referencing. There is, however, no laser medium with a gain spectrum spanning a full octave: the gain profile approaches a half-octave for Ti:sapphire, for example. Thus, nonlinear effect must be exploited for broadening the output spectrum of the

mode-locked laser. A photonic crystal optical fiber is widely employed as a nonlinear optics for the production of the spectrum more than an octave of bandwidth[8]. The photonic fiber has a microstructure consisting of regularly spaced air holes. They allow the creation of waveguides that strongly confine the light field to a small area and control the zero dispersion point of the fiber close to the center wavelength of the mode-locked laser employed; high peak intensity and long effective length of the nonlinear interaction in the fiber. These features result in a strong self-phase modulation (SPM) that can provide a broadband spectrum over an octave. Although the photonic fiber has facilitated to obtain the octave-spanning optical comb, there exist some disadvantages for using it:

- coupling the light into the fiber is alignment sensitive and tends to degrade with time because of the small core of the fiber.
- small core of the fiber results in the damage due to the high peak intensity.
- excess phase noise is appeared in the light transmitted through the fiber[9].

These could be serious problem for the establishment of optical standard requiring the stable long-term operation, good reproducibility, and high-precision frequency measurements.

The mode-locked solid-state lasers directly emitting the broadband spectrum[10] and mode-locked fiber lasers can overcome the drawbacks concerning the photonic fiber. The former lasers exploit the nonlinearity of the laser crystal to generate spectral components outside of the gain region. It is due to the SPM in the laser crystal and avoids the issues of coupling and damage to the fiber. Such lasers must be carefully designed to generate ultra-short pulses by the compensation of the group-velocity dispersion in the laser cavity. To achieve a high reflectivity and compensation of the group delay simultaneously, chirped mirrors are often employed instead of intracavity prisms[11]. This leads compactness of the laser cavity, which can enhance the mechanical stability and achieve high repetition rate of pulses.

The high f_{rep} plays an important role for a heterodyne beat measurement with good signal-to-noise ratio (SNR) because of a higher power per mode at the same average output power. It also yields a good beat signal separation from the neighboring comb modes. However, the power per pulse decreases as the repetition rate increased. This should be considered when one is to rely on the nonlinear processes to broaden the optical spectrum to an octave.

The development of the mode-locked fiber lasers has experienced an extraordinary growth due to the significant role in the high-speed optic-fiber communications. The rare-earth-doped optical fibers are employed for their gain medium. They are capable of emitting the ultra-short optical pulses in sub-fs range. The fiber-based FLFCs are attractive devices due to their advantages: small size, low cost and transportability. In particular, erbium (Er)-fiber laser based optical comb have a mechanically stable all-fiber design by using a wavelength division multiplexing (WDM) coupler for pump light coupling. This read the unprecedented long-term operation over weeks[12]. Regarding the phase noise caused by the pulse spectrum broadening in the nonlinear fiber, strenuous efforts have enabled to reduce it at the no significant level[13][14]. However, there still exists a few drawbacks; typical f_{rep} of the fiber lasers is lower than that of Ti:sapphire lasers. The wavelength conversion must be applied to access the optical clock transitions, which mostly range from the visible to near-infrared regions.

2.2 Optical frequency measurement using femtosecond laser frequency combs

The laser frequency f_{cw} measured can be determined by measuring the heterodyne beat frequency f_{beat} between the laser and n -th mode of FLFC with a frequency $f(n)$ closest to the laser frequency. Then f_{cw} is given by

$$f_{\text{CW}} = f(n) \pm f_{\text{beat}} \quad (5)$$

where the plus sign holds for the higher f_{cw} than $f(n)$, the minus sign for the lower f_{cw}

than $f(n)$. Since $f(n)$ is written by

$$f(n) = nf_{\text{rep}} \pm f_{\text{ceo}} \quad (6)$$

one must decide the both sign for the f_{beat} and f_{ceo} as well as the integer n in the measurement[15]. The procedure is as followings: step1: determination of sign for f_{beat} , step2: determination of sign for f_{ceo} , and step3: determination of n .

The sign of f_{beat} represents the magnitude relation between the $f(n)$ and f_{cw} . It can be decided by observing the increase and decrease in f_{beat} as the f_{rep} is changed:

$$A \equiv \frac{\partial f_{\text{beat}}}{\partial f_{\text{rep}}} = \begin{cases} > 0 & \rightarrow f_{\text{cw}} < f(n) \\ < 0 & \rightarrow f_{\text{cw}} > f(n) \end{cases} \quad (7)$$

Once the sign for f_{beat} is fixed, one can determine the sign for f_{ceo} . Here, we define the frequency of the beat signal, F_{ceo} ($0 \leq F_{\text{ceo}} \leq f_{\text{rep}}/2$), measured by the self-referencing interferometer. The $f(n)$ is changed as the F_{ceo} is increased and decreased:

$$B \equiv \frac{\partial f(n)}{\partial F_{\text{ceo}}} = \begin{cases} > 0 & \rightarrow f_{\text{ceo}} > 0 \\ < 0 & \rightarrow f_{\text{ceo}} < 0 \end{cases} \quad (8)$$

From the Eq.(7) and (8), f_{cw} is classified into any four cases:

$$f_{\text{CW}} = \begin{cases} nf_{\text{rep}} + f_{\text{ceo}} - f_{\text{beat}} & \text{sgn}(A) = \text{sgn}(B) = 1 \\ nf_{\text{rep}} - f_{\text{ceo}} - f_{\text{beat}} & \text{sgn}(A) = 1, \text{sgn}(B) = -1 \\ nf_{\text{rep}} + f_{\text{ceo}} + f_{\text{beat}} & \text{sgn}(A) = -1, \text{sgn}(B) = 1 \\ nf_{\text{rep}} - f_{\text{ceo}} + f_{\text{beat}} & \text{sgn}(A) = \text{sgn}(B) = -1 \end{cases} \quad (9)$$

where $\text{sgn}(x)$ is a sign function. It is defined simply as 1 for $x > 0$ and -1 for $x < 0$. Considering the signs for f_{beat} and f_{ceo} , the integer n can be determined by

$$n = \frac{f_{\text{CW}} \pm f_{\text{ceo}} \pm f_{\text{beat}}}{f_{\text{rep}}} \quad (10)$$

Commercial wavelength meters can measure the f_{cw} with an accuracy of less than 1 ppm, which is usually sufficient for the determination of the last whole digit of n : for instance, when the numerator of the right-hand side of Eq.(10) and f_{rep} in the denomination are as-

sumed to be 400 THz and 1 GHz respectively, the required resolution for the wavelength meter is 7 digits.

The uncertainty of the measured absolute frequency of the laser is restricted by that of a microwave standard referenced by the FLFC. The microwave reference must be compared with the Coordinated Universal Time (UTC) to correct its frequency. The Circular T, a monthly bulletin distributed from the International Bureau of Weights and measures (BIPM), reports the UTC calculated by the BIPM and the deviations of local time scales for each national institutes and the system times used for the Global Positioning System (GPS). In the national institutes or having a link with the GPS, one can maintain the uncertainty of the microwave reference as well as that of the UTC^[16].

3 Development of femtosecond laser frequency combs

The FLFCs in NICT are required the measurement accuracy of 10^{-16} level. They must be stably operated more than 8 hours for at least 5 days to compare the optical standards and microwave ones. In order to satisfy these requirements, we developed the FLFCs based on Kerr-lens mode-locked fs-pulse Ti:sapphire lasers directly emitting broadband continuum: Venteon OS (Nanolayers) and Gigajet 20W (Gigaoptics). Table 1 summarizes their specifications. In this section, we describe their optical and control systems. A fiber-based FLFC recently developed is also presented.

Table 1 Specifications of the femtosecond-pulse mode-locked Ti:sapphire laser applied in the present research

	Venteon OS	Gigajet 20W
Output power (mW)	200	800
Repetition rate (MHz)	200	1000
Pulse length (fs)	< 8	26
Spectral coverage (nm)	600 ~ 1280	630 ~ 990

Specifications of femtosecond-pulse mode-locked Ti:sapphire lasers we employed for the development of the optical frequency counters. The measured values are described in romans, whereas the nominal value from the data sheet is written in *italics*.

3.1 Venteon OS femtosecond-pulse laser frequency comb (NICT-FCB1)

3.1.1 Venteon OS and f-to-2f self-referencing interferometer

Venteon OS is a Kerr-lens mode-locked Ti:sapphire laser generating fs pulses with the f_{rep} of 200 MHz^[17]. It consists of a z-folded cavity, Ti:sapphire laser crystal and three BaF₂ plates as illustrated in Fig. 2. The double-chirped mirrors constituting the cavity can generate the negative dispersion for compensation of the positive dispersion caused by the laser crystal and the air path. The BaF₂ plates also serve as the dispersion compensation optics for reduction of the pulse width less than 8 fs, since it has the lowest ratio of third- to second-order dispersion in the wavelength range from 600 to 1200 nm. Figure 3 depicts the output spectrum observed. The broadband spectrum extending from 600 nm to 1280 nm at -20 dB below the

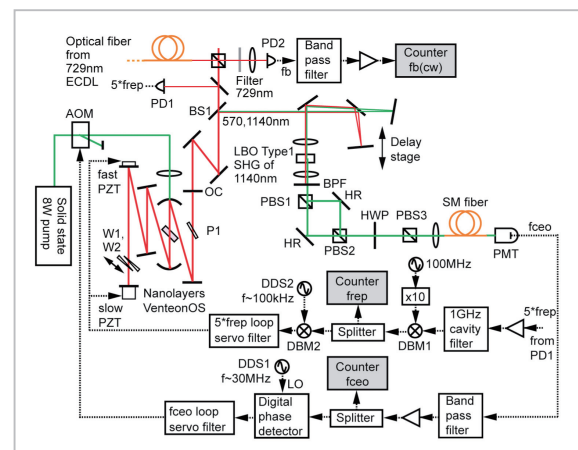


Fig.2 Optical frequency with Venteon OS femtosecond laser comb

Experimental setup of optical frequency comb based on 200 MHz octave-spanning Ti:sapphire laser Venteon OS (NICT-FCB1). AOM: acousto-optical modulator, DDS: direct-digital synthesizer, DBM: double-balanced mixer, HWP: half-wave plate, LBO: LiB₃O₅ crystal, LO: local oscillator, PBS: polarizing beamsplitter, PD: photodiode, PMT: photomultiplier tube, SM fiber: single-mode fiber, PZT: piezo-electric transducer, OC: output coupling mirror, P1: BaF₂ plate, W1, W2: BaF₂ wedge. Note that all DDSs and frequency counters are referenced to a hydrogen maser, although it is not shown in this figure.

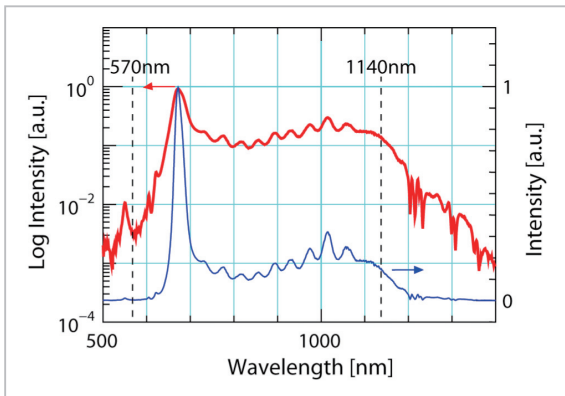


Fig.3 Output spectra of Venteon OS

Output spectrum of Venteon OS femtosecond-pulse mode-locked laser on a linear (blue thin line) and logarithmic scale (red bold line). The wavelength of 570 nm and 1140 nm are indicated by two dotted lines.

maximum is reached one octave and sufficient for accessing to f_{ceo} without external spectral broadening. The average output power was measured to be 200 mW, when the laser was pumped by a frequency doubled Nd:YVO₄ laser with an output power of 5.7 W at 532 nm in wavelength.

The spectral components around 570 and 1140 nm were applied to the self-referencing technique. These were separated from a main output beam by a dichroic beamsplitter (BS1) and introduced into an f-to-2f self-referencing interferometer. The fundamental design of the interferometer is similar to one described in Ref.[17] but slightly modified for the inferior beam profile of our laser. The spectral components around 1140 nm were frequency-doubled in a SHG non-linear LiB₃O₅ crystal with a thickness of 2 mm, and then it was overlapped to the components around 570 nm. An optical delay line was included in the infrared part to temporally overlap the pulse electric fields. Additionally, we employed a Mach-Zehnder-like interferometer to spatially superimpose two beams at 570 nm, because the spatial mode of each beam had large discrepancy. In order to decrease the shot noise, an optical bandpass filter is employed to transmit the light contributing the f_{ceo} signal detection. Both green lights transmitted through a single-mode (SM) fiber

for the rejection of higher-order spatial modes were detected by a photomultiplier tube. The f_{ceo} beatnote signal was observed with a signal-to-noise ratio (SNR) of more than 35 dB in a 300 kHz of resolution bandwidth (RBW) of rf spectrum analyzer. On the other hand, a fraction of the main beam was picked-off and directly detected for the f_{rep} counting by a fast photodetector (PD1).

3.1.2 Frequency control systems

The f_{ceo} stabilization was achieved by a phase-locked loop (PLL). The beatnote frequency corresponding to f_{ceo} was passed through a tunable bandpass filter, amplified, and then compared with a local oscillator of 30 MHz by using a digital phase detector after being divided by 4[18]. The local oscillator signal was supplied by a direct-digital synthesizer (DDS1) externally referencing to a hydrogen maser (H-maser). The control signal was fed back to an acousto-optical modulator (AOM) placed in the pump beam, which regulates the pump intensity and thus modifies the f_{ceo} by changing the optical path length in the laser crystal via its optical Kerr effect. The control bandwidth was measured to be 5 kHz in Fourier frequency. The feedback gain achieved was more than 160 dB below 1 Hz. The CE offset phase noise was 2×10^6 rad/Hz^{1/2} at 1 Hz in free running. It was suppressed down to 3×10^{-4} rad/Hz^{1/2} with the PLL. The residual fluctuation of f_{ceo} was monitored by an rf counter and found to be less than 1 mHz in 1-s gate time. It was equivalent to the measurement accuracy of 10^{-18} level.

The 5th harmonic of f_{rep} at approximately 1 GHz was detected to extract a control signal for the f_{rep} stabilization. This manner reduces the phase noise multiplication to the optical frequency[19][20]. The control signal was obtained by two down-conversion steps. In the first step, the 5th harmonic of f_{rep} was down-converted into an intermediate frequency by mixing with a frequency reference at 1 GHz, which was produced from a 100 MHz output of the H-maser by electrically frequency multiplication. The intermediate frequency at a typically hundred kHz was again compared with an output of DDS2 to yield the control signal. The

low-frequency components of the signal are directed toward the slow PZT attached to the laser mirrors to stabilize the cavity length fluctuation. The high-frequency components are fed back to the fast PZT to expand the control bandwidth of the PLL. The unity gain and crossover frequency of the two feedback paths were 500 Hz and 50 Hz, respectively. From the intermediate frequency counting, the instability of f_{rep} was evaluated to be as low as 1×10^{-14} at 1 s averaging time. It was restricted by a resolution of the rf counting equipment.

3.2 Gigajet 20W femtosecond-pulse laser frequency comb (NICT-FCB2)

3.2.1 Gigajet 20W and 2f-to-3f self-referencing interferometer

Gigajet 20W is a Kerr-lens mode-locked Ti:sapphire laser with a repetition rate of 1 GHz [21]. As illustrated in Fig. 4, the laser cavity forms a bow-tie shape, which is comprised of two concave and one convex chirped mirrors, and an output coupler. A laser crystal is located at Brewster angle between the con-

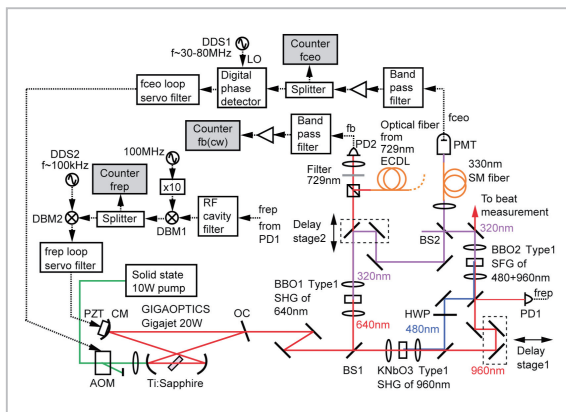


Fig.4 Optical frequency combs with Gigajet 20W femtosecond laser

Experimental setup of optical frequency comb based on Gigajet 20W (NICT-FCB2). PD: photodiode, DBM: double-balanced mixer, DDS: direct-digital synthesizer, PZT: piezoelectric transducer, AOM: acousto-optic transducer, HWP: half-wave plate, BBO: β -barium-borate crystal, OC: output coupling mirror, CM: convex mirror, BS: beamsplitter, PMT: photomultiplier tube, SM fiber: single-mode fiber. Counters and DDSs have common rf-reference, although it is not illustrated in here.

cave mirrors. The average output power was 800 mW at the pumping power of 8.5 W. The pulse width was measured to be 26 fs. Figure 5 shows a typical output pulse spectrum. It ranges from 630 to 990 nm at 20 dB below the maximum.

We employed the complicated 2f-to-3f self-referencing techniques, since the spectrum coverage was not enough to observe the f_{ceo} with a high SNR by the conventional self-referencing. The design of a 2f-to-3f interferometer borrowed heavily from one previously reported by Ramond et al [22]. A BS1 reflected the spectrum below 740 nm into a SHG arm of the interferometer, whereas the remainder of the spectrum was transmitted and introduced into a third-harmonic generation (THG) arm. In the SHG arm, the spectral components around 640 nm were frequency-doubled to produce a 320 nm light by using a Type I β -barium-borate1 (BBO1) crystal with the 0.3 mm thick. In the THG arm, the spectral components around 960 nm were frequency-tripled in two steps to also produce 320 nm light; a KNbO₃ generated the SHG of 960 nm at first, and next BBO2 in the THG arm produced the 320 nm light by the sum-frequency generation of the 480 and 960 nm. The 320 nm ultraviolet (UV)

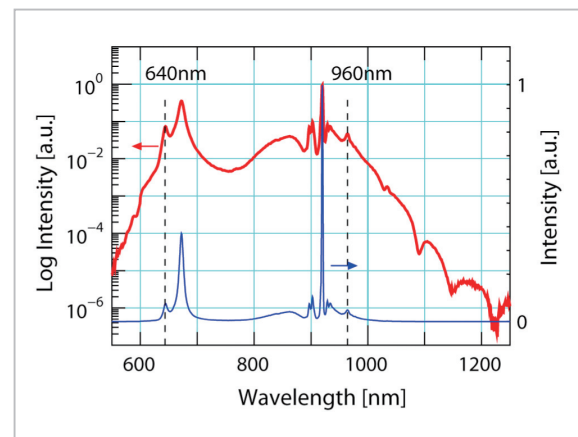


Fig.5 Output spectra of Gigajet 20W

Output spectrum of Gigajet 20W mode-locked laser on a linear (blue thin line) and logarithmic scale (red bold line). The spectral components at 640 and 960 nm are used for the 2f-to-3f self-referencing technique (indicated by the two dotted lines).

light from both arms were interfered on the BS2 to obtain f_{ceo} : the beat frequency $3f(n) - 2f(m) = 3(nf_{\text{rep}} + f_{\text{ceo}}) - 2(mf_{\text{rep}} + f_{\text{ceo}}) = f_{\text{ceo}}$ with $m = 3n/2$. To observe the f_{ceo} signal with high SNR, the two pulsed beams must have the same polarization and must overlap temporally, spectrally and spatially. Temporal overlap is achieved by means of a delay stage 2 in the SHG arm. Spectral overlap within the accuracy of 1 nm wavelength is obtained by angle tuning of the nonlinear crystals and is verified with an optical spectrometer. Spectral overlap is accomplished by use of UV SM fiber with spatial filtering. Since the UV light power transmitting the fiber was only several tens nanowatts, we used a photomultiplier tube for the high-efficiency detection. The f_{ceo} beatnote signal typically had a SNR of 30 dB in a 300 kHz RBW. Such high SNR in the 2f-to-3f interferometer was achievable by the best mode matching of the UV light from the THG arm into the SM fiber rather than the light from the SHG arm. The f_{rep} was monitored by a fast PD1 with detecting a small part of the laser output.

3.2.2 Frequency control systems

The control schemes of f_{ceo} and f_{rep} of NICT-FCB2 are similar to those of NICT-FCB1. The f_{ceo} obtained by the 2f-to-3f self-referencing technique was bandpass-filtered and then down-converted with a local oscillator to extract the control signal. The local oscillator was a DDS1 with the same external rf reference as used in NICT-FCB1. The signal was appropriately filter-amplified by a servo electronics and fed back to an AOM for modulating the pump power. The f_{ceo} control bandwidth was about 40 kHz, which was restricted by the frequency response of the AOM. The residual frequency fluctuation measured by a frequency counter was less than 10 mHz, which corresponds to 10^{-17} level at 1-s averaging time in optical frequency.

The pulse repetition rate of 1 GHz was used to stabilize the f_{rep} . The control signal was fed back to a PZT attached to the convex mirror. The control bandwidth was adjusted to be about 1 kHz to exploit the intrinsic stability of the laser cavity at the high frequencies. The stability

of f_{rep} was reached at least 5×10^{-15} at the averaging time of 1 s, which was dominated by the counter resolution.

3.3 Erbium-fiber mode-locked laser based frequency comb (NICT-FCF1)

3.3.1 Erbium-fiber laser and optics

NICT-FCF1 is composed of three major components: an Er-doped-fiber mode-locked laser, a self-referencing interferometer arm and a frequency measurement arm. The Er-fiber laser has an all-fiber ring resonator including a polarization sensitive isolator, an output coupler, a polarizer and a WDM coupler for pumping the Er fiber with the 980 nm diode laser[23]. An in-line polarization controller containing a half-wave and quarter-wave plates is also set in the cavity for ensuring the mode-locking operation. The nonlinear polarization rotation is employed as the mode-locking mechanism. It is the intensity-dependent change in the state of polarization of a single pulse propagating inside an optical fiber[24]. The physical mechanism behind the mode locking is similar to that of the Kerr shutters for the NICT-FCB1 and -FCB2; a linearly polarized pulse just after the isolator is rotated during the propagation by the intensity dependence of the nonlinear phase shift imposed on the orthogonal polarized components of the pulse electric fields. The polarizer appropriately adjusted lets the central intense part of the pulse pass but blocks the low-intensity pulse wings. The net result is that the pulse is slightly shortened after one round trip inside the ring resonator. The pulse width was measured to be 351 fs with the f_{rep} of 55 MHz. Figure 7(a) shows the output pulse spectrum with the typical average output power of 5 mW. The center wavelength and spectral width were 1557 nm and 14 nm, respectively. The output spectrum exhibited the Kelly sidebands, which was caused by the chirped soliton circulating inside the cavity with the periodic perturbations on the soliton energy [25]. This laser is capable of turnkey operation.

The fiber-laser output was splitted by a 3 dB fiber coupler and then introduced into the

self-referencing interferometer arm and the frequency measurement arm [26]. The optical pulses in the self-referencing arm were amplified to the 90 mW average output power by an erbium-doped fiber amplifier (EDFA). The output of the EDFA was launched into a highly nonlinear fiber (HNLf) to broaden the spec-

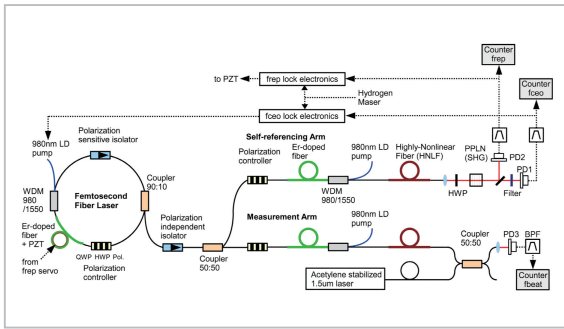


Fig.6 Er: fiber mode-locked laser optical frequency combs

Experimental setup of optical frequency comb based on Er: fiber mode-locked laser (NICT-FCF1). PD: photodiode, PZT: piezo-electric transducer, HWP: half-wave plate, PPLN: periodically poled lithium niobate crystal, WDM: wavelength-division multiplexing coupler. Counters have common rf-reference, although it is not illustrated in here.

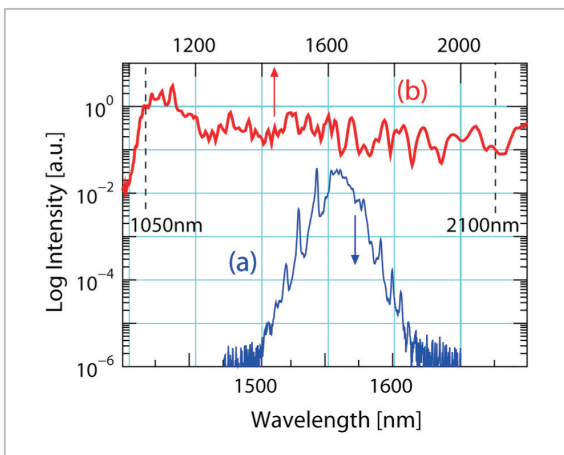


Fig.7 Output spectra of the mode-locked fiber laser

Output spectra of Er: fiber mode-locked laser before (blue line) and after highly nonlinear fiber (red bold line). The spectral components at 1050 and 2100 nm are used for the self-referencing technique (indicated by the two dotted lines).

trum of the optical pulses as a result of nonlinear effect such as SPM. The HNLf with the 40 cm length has a zero dispersion wavelength of 1539 nm, a nonlinear coefficient of about 20 W/km. The incident pulse to the EDFA was negatively pre-chirped by a SM fiber with the appropriate length to compensate the positive chirped pulse in the EDFA, consequently the octave-spanning spectrum is induced by the strong nonlinear effect in the HNLf. The broadened spectrum after the HNLf is shown in Fig. 7(b). It covers a wavelength range of 1 μm to more than 2.2 μm . The f_{ceo} was detected by the common-path self-referencing interferometer. The component around 2100 nm is frequency-doubled by the periodically poled lithium niobate (PPLN) crystal with the 1 mm length and mixed with the component around 1050 nm on the PD1. The SNR of f_{ceo} beatnote was 35 dB with the RBW of 300 kHz. This interferometer has simplicity and robustness, however it requires to adjust the length of the fiber fused after the HNLf for temporal overlapping of the two 1050 nm beams. The f_{rep} signal was obtained by the direct detection of pulse train with the PD2.

3.3.2 Frequency control systems

The f_{ceo} was stabilized by the PLL to the 21 MHz signal generated from the DDS, which is referenced to the H-Maser. Its control signal was fed back to the LD current to modulate the pump power for the laser oscillator. The control bandwidth was 20 kHz and the feedback gain was achieved to be 200 dB at 1 Hz. The relative frequency fluctuation of f_{ceo} was less than 10 mHz in 1 s counter-gate time.

The 18th harmonic of f_{rep} was detected to extract its control signal. The signal was directed toward the cylinder-shaped PZT wound with Er-doped fiber for changing the cavity length. The PZT has a large diameter of 60 mm to prevent the bending loss in the fiber. The unity gain frequency of the feedback loop was approximately 200 Hz, which was restricted by the first mechanical resonance of the PZT. The actuator had a dynamic range of about 400 Hz that is sufficient for the continuous operation of over several days, when the laser cavity is tem-

perature-controlled.

4 Precise frequency measurements with femtosecond laser frequency combs

In this chapter, we present the performance of NICT-FCB1 and -FCB2. The basic scheme of our measurements is to compare pair of FLFCs and verify with the consistency of absolute frequencies measured by each FLFC, photodetection of f_{rep} and optical heterodyne technique, in which the f_{rep} and the output modes have their expected frequencies relative to a reference laser. We introduce the long-term measurement of a 1.5 μm laser for the optical-fiber communications with NICT-FCF1.

4.1 Performance of the broadband Ti:sapphire laser frequency combs

Figure 8 illustrates the experimental setup for the comparison of absolute frequencies measured by NICT-FCB1 and -FCB2 [27]. They count the frequency of one cw laser, simultaneously. The frequencies f_{cw1} and f_{cw2} measured by NICT-FCB1 and -FCB2 respectively are given by

$$f_{\text{cw1}} = n_1 f_{\text{rep1}} + f_{\text{ceo1}} + f_{\text{beat1}} \quad (11)$$

$$f_{\text{cw2}} = n_2 f_{\text{rep2}} + f_{\text{ceo2}} + f_{\text{beat2}} \quad (12)$$

where the subscripts 1 and 2 denote the corresponding FLFCs. Since both absolute frequencies should be equal $f_{\text{cw1}} = f_{\text{cw2}}$, the frequency difference between two measurements $\Delta f \equiv f_{\text{cw2}} - f_{\text{cw1}}$ indicates the potential limitation in FLFCs. The frequency difference can be given by

$$\Delta f = f_2(n_2) - f_1(n_1) + \Delta f_{\text{beat}} \quad (13)$$

where $\Delta f_{\text{beat}} \equiv f_{\text{beat2}} - f_{\text{beat1}}$. The $f_1(n_1)$ and $f_2(n_2)$ can be determined precisely, whereas the Δf_{beat} is obtained by mixing two heterodyne beatnotes and measurable by an rf counter. The sign of Δf_{beat} is found out in the measurement.

A cavity-stabilized diode laser oscillating at 729 nm in wavelength was employed for this comparison [28]. The laser beam was split by a 3 dB fiber coupler and then distributed by polarization-maintained SM fibers for heterodyne detection with each FLFC. The SNR of the heterodyne beatnotes were kept more than 33 dB

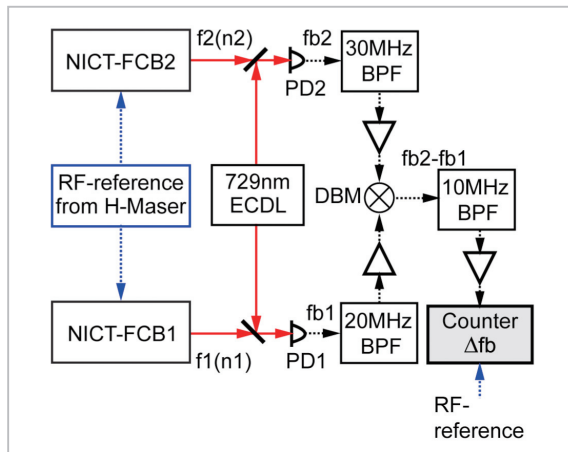


Fig.8 Experimental setup for the measuring performance evaluation with two optical frequency combs

Experimental setup for the comparison of absolute frequencies measured by two FLFCs. PD: photodiode, DBM: double-balanced mixer, BPF: band-pass filter, ECDL: extended cavity diode laser. The triangles indicate rf amplifiers.

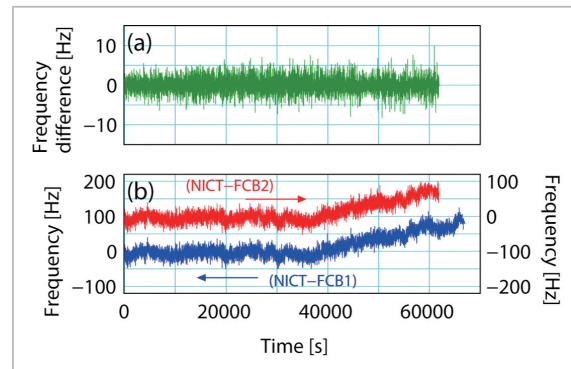


Fig.9 Laser absolute frequencies measured by two optical frequency combs (b) and their differences (a)

(a) Difference of absolute frequencies measured by two independent FLFCs. (b) The blue and red lines represent the absolute frequencies measured by NICT-FCB1 and -FCB2, respectively. Both are in good agreement. The frequency offset of 411 041 304 103 330 Hz and drift at a rate of 45 mHz/s are subtracted from the absolute frequencies.

with an RBW of 300 kHz over 16 h. The frequency miscounting caused by the SNR degradation was not occurred during this measurement. The clock laser powers required were $150 \mu\text{W}$ to satisfy the SNR. The $f_{\text{beat}1}$ and $f_{\text{beat}2}$ were set to be about 20 and 30 MHz, and filtered through elliptic-frequency-response bandpass filters with -1.5 dB bandwidth of 4.4 and 6 MHz respectively. Both were mixed to generate the Δf_{beat} by a double-balanced mixer. The Δf_{beat} about 10 MHz was again bandpass-filtered to improve the measurement precision before the counting. The filter had also the elliptic response and narrower 2 MHz bandwidth. Figure 9(b) shows the two independent frequency measurement with 10 s counter gate time. A frequency offset of 411 041 304 103 330 Hz and constant frequency drift at a rate of 45 mHz/s were subtracted from the absolute frequency measured for convenience. The blue and red plots indicate the results obtained by NICT-FCB1 and -FCB2, respectively. Both results are in fairly good agreement. The cycle slips in PLLs for f_{rep} and f_{ceo} of each FLFCs were detected by monitoring their frequencies using separate counters and removed from the plots. The amplitude of frequency fluctuation was limited by the stability of the rf-reference from the H-maser. The frequency drift subtracted and excursion were mainly originated from the stabilized laser. Uninterrupted long-term operations of both FLFCs were attained over 16 h. The frequency difference Δf between the two measurements is plotted in Fig. 9(a). The cycle slips on the PLLs and frequency miscounting of Δf_{beat} due to the frequency deviations exceeding a bandwidth of the 10 MHz bandpass filter were rejected from the plot. The frequency fluctuation originated from the rf-reference and large drift caused by the stabilized laser were canceled out in the mixing process. In this measurement, the mean of the frequency difference and a standard error were calculated to be 25 ± 26 mHz, respectively. The frequency offset was found to be mainly originated from the Δf_{beat} miscounting.

The instability of FLFCs must be evaluated to give the rigorous limitations on characteriza-

tion of the statistical frequency fluctuation of optical standards. Figure 10 plots the Allan deviations derived from the two independent frequency measurements and their difference in Fig. 9. The Allan deviation of two measurements was equivalent. They started at 3×10^{-14} at the averaging time of 10 s and drops until 100 s, which was caused by the instability of the rf-reference distributed from the H-maser. The influence of the linear frequency drift caused by the cavity-stabilized laser is observed for the averaging time longer than 100 s. The Allan deviation of the Δf was 5×10^{-15} at 10 s and averaged down to 10^{-17} level with a dependence of $\tau^{1/2}$ (Fig. 10(d)). The frequency fluctuations caused by the rf-reference and stabilized laser were rejected as the common-mode noise. The Allan deviation indicates the potential to reach the relative frequency stability of two FLFCs lower than 1×10^{-16} within 3×10^4 s. One possibility for this limitation was the reduction of relative coherence of two FLFCs referencing to the common microwave standard. Such reduction could be caused by incoherent phase noise in the PLLs, which enter in

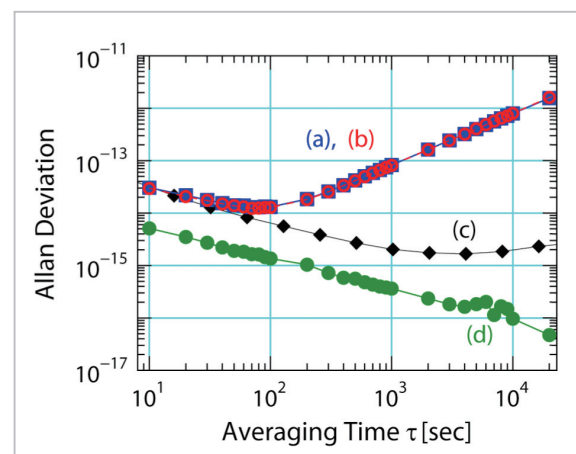


Fig. 10 Laser frequency stabilities measured by two optical frequency combs

Measured frequency instabilities as given by the Allan standard deviation. (a, b) Instabilities of 729 nm frequency-stabilized laser measured by NICT-FCB1 and -FCB2, respectively. (c) Instability of hydrogen maser employed as rf-reference. (d) Relative instabilities of two FLFCs obtained from the difference of the two independent frequency measurement.

the output of FLFCs under the multiplication of the microwave to optical frequencies[29][30]. Another was the excess phase noise from the photodiodes extracting the f_{rep} signals. The noise were related to the power-to-phase conversion in the photodiodes, which especially arose with the detection process of ultrashort light pulses[31][32].

The comparison with cesium microwave standards at the accuracy approaching 10^{-16} range usually takes over several days. The reproducibility of frequency measurement features largely in the definition of new SI second. In our optical standards, the FLFCs are required the reproducible high-precision measurements during 5 days in addition to the continuous operation exceeding 8 hours for each measurement. This is because the frequencies measured for at least 5 days must be averaged to be compared with the UTC and the typical operation period of the optical standard for one measurement set is planed to be 8 h for deriving the absolute frequency with the uncertainty of 10^{-15} level, that is restricted by the microwave standard. Considering the above situation, we have repeatedly compared two FLFCs on 5 days within 2 weeks. This is adequate to investigate their reproducibility over 5 days, although the comparisons were not implemented continuously for 5 days. Figure 11 shows a summary of the absolute frequency comparison. The difference between the frequencies measured are plotted with the total averaging time T and the 10 s Allan standard deviation σ_y for each comparison. The daily measurements were carried out with the different f_{rep} and f_{ceo} for each FLFC. The all means of data sets were within the fractional difference of 1.2×10^{-16} , thus the FLFCs were ensured to have good reproducibility. The weighted mean of all data from 5 days was calculated to be 7.6×10^{-17} with a standard error of 2.8×10^{-17} . We found that average frequencies measured by two FLFCs agree within the uncertainty of 8.1×10^{-17} . The FLFCs developed enable to compare the optical frequencies against a cesium atomic fountain clock with the best uncertainty under their reliable long-term operation[33]. It should be

noted that the maintenance of the FLFCs was hardly required for the continuous operations over 8 hours during the repeated comparisons. Such reliable operation was allowed by the broadband fs lasers without PCFs and was essential for the FLFCs as optical frequency counters.

In the above, we have reported the performance of the so-called microwave-to-optical synthesizer based on FLFCs, in which FLFCs are used as a frequency up-converter of the microwave standard to the optical region. By the way, FLFCs can be viewed as a general purpose extremely broadband synthesizer with either an optical or microwave frequency reference. An optical-to-microwave frequency synthesizer is employed to down-convert the laser frequency into microwave. The microwave synthesis from stabilized laser potentially achieves high stability sufficient for Ramsey spectroscopy in the cesium atomic fountain clocks and thus it is applicable for optical clockwork. An optical-to-optical frequency synthesizer is able to bridge the large optical frequency intervals and compare optical clocks made from different atomic species. For these purposes, the n -th component $f(n)$ of the FLFC

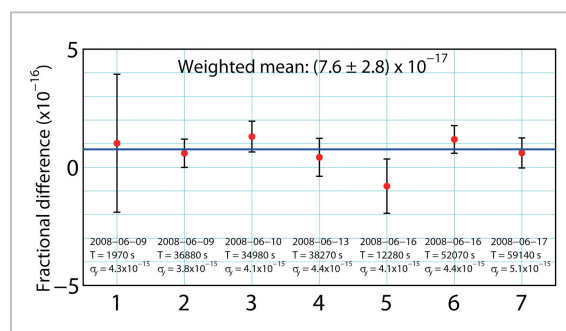


Fig. 11 Results for measurements of laser absolute frequency with two optical frequency combs

Summary of the comparison of absolute frequency measurements. The weighted mean of all data is calculated to be $(7.6 \pm 2.8) \times 10^{-17}$ and is shown by a blue line. The total averaging time (T) and the 10 s Allan standard deviation (σ_y) are also written for each comparison. Note that a mean of the first data set has a larger standard error because of the shorter averaging time.

must be stabilized to the reference laser f_{cw} by the phase locking of f_{beat} to a microwave reference, and f_{ceo} is also locked to a microwave standard. Then f_{rep} is phase coherently linked to f_{cw} as

$$f_{rep} = \frac{1}{n}(f_{cw} - f_{beat} - f_{ceo}) \quad (14)$$

If we redefine the origin of the comb, we can now rewrite Eq. (3) as

$$f(k) = f_{cw} - f_{beat} \pm \frac{k}{n}(f_{cw} - f_{beat} - f_{ceo}) \quad (15)$$

(k: any integer)

In this expression, the effective origin of the FLFC is f_{cw} and the f_{rep} is always given by Eq. (14). Thus, all optical frequencies $f(k)$ as well as f_{rep} are phase locked to f_{cw} . More generally, both accuracy and stability of f_{rep} and $f(k)$ are determined entirely by f_{cw} even if f_{ceo} and f_{beat} are referenced to the microwave standards.

In optical-to-microwave frequency synthesizer, the optically referenced pulse train at f_{rep} must be converted to an electronic microwave signal using a fast photodiode. It has been previously mentioned that the excess power-to-phase noise was added to the microwave sig-

nal in the conversion process. Therefore, it is worthwhile to investigate the possible influence of the noise on the uncertainty of f_{rep} for the applications such as the radar, deep space navigation, VLBI and optical clock. Figure 12(A) illustrates the experimental setup for the comparison of f_{rep} by the photodiode detection. The both heterodyne beat f_{beat1} and f_{beat2} were phase locked to the frequency-stabilized reference laser, while the f_{ceo1} and f_{ceo2} were phase locked to the output of DDSs having external frequency reference from H-maser (not shown in the figure). The optical pulse trains from each FLFC were detected by PD1 and PD2, and converted to the microwave signals at f_{rep1} and f_{rep2} . The dual mixer time difference method was employed for the phase comparison of the 5th harmonics of f_{rep1} and fundamental of f_{rep2} . The relative fractional instability to the optically referenced laser was 2×10^{-14} at 1 s as shown in Fig. 13(a). We suppose the instability was limited by the power-to-phase conversion noise, since it agreed with the relative instability of the microwave-to-optical synthesizer configuration (Fig. 10(d)); both are sensitive to the influence of the excess phase noise. The relative fractional frequency difference between two FLFCs was 2.2×10^{-17} with an uncertainty of 8.7×10^{-17} within the measurement time of 2800 s. This uncertainty is no significant level

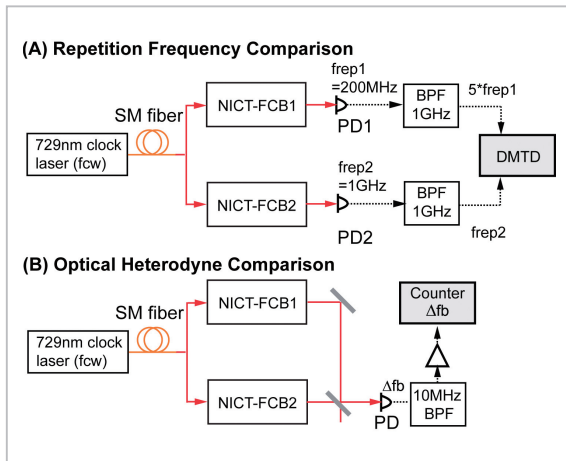


Fig. 12 Comparative experiment between light-microwave and light-optical synthesizer with NICT-FCB1 and -FCB2

Experimental setup for the repetition frequency comparison and optical heterodyne comparison by two FLFCs.

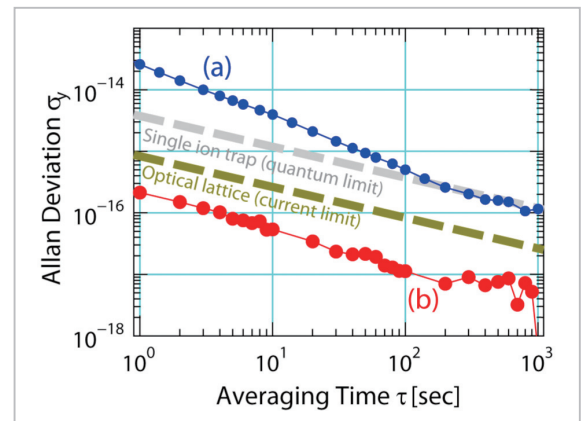


Fig. 13 Relative frequency stabilities between light-microwave (a) and light-optical synthesizer (b) with NICT-FCB1 and -FCB2

Relative instabilities of two FLFCs obtained from the repetition frequency comparison (a) and optical heterodyne comparison (b).

to compare the frequency of optical clocks to the current-best primary frequency standard in the microwave region.

The high-frequency noise of the free-running local oscillator is appeared in the output of the frequency standards and is often degraded the frequency stability expected. This, so-called the Dick effect, is caused by the demodulation process in the modulation techniques needed for the stabilization of the local oscillator to a passive reference. The phase noise measurement of the f_{rep} is required to identify the Dick noise level in the frequency stability of the primary standards operating with the optical clockwork. Figure 14 displays the single-sideband (SSB) phase-noise spectrum of several rf oscillators. The 1 GHz signal down-converted from the cavity-stabilized laser frequency by using NICT-FCB2 is plotted in Fig. 14(b). The SSB phase noise level was -145 dBc/Hz at 10 kHz from the 1 GHz carrier frequency, which was 60 dB lower than that of the commercially available oscillator (Fig. 14(a)). Clearly, there is a large potential payoff in the phase noise level offered stabilized laser com-

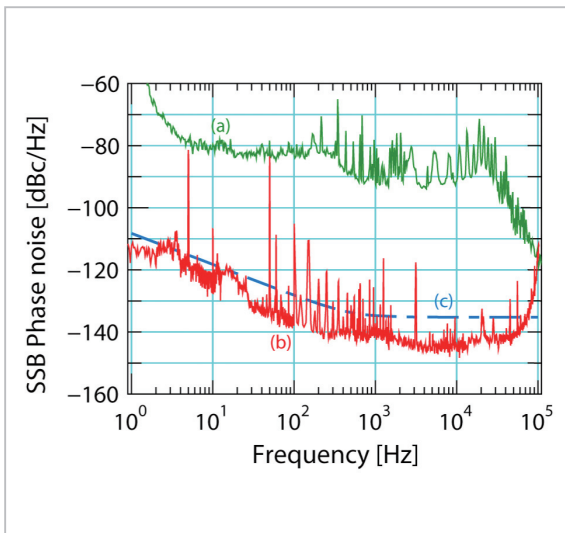


Fig.14 Phase noise spectra of the 1 GHz signal from various cavities and synthesizers

Single-sideband phase noise spectra of various oscillators and synthesizers at 1 GHz. (a) SSB phase noise spectrum of commercial rf oscillator, (b) 1 GHz signal produced from 729 nm ECDL and (c) cryogenic sapphire oscillator[35].

pared to a cryogenic sapphire oscillator (CSO) (Fig. 14(c)), which is the best existing microwave source[36]. Recently, cesium atomic fountain primary frequency standards in two metrology institutes have been actually operated with the low-phase-noise local oscillator composed of the cavity-stabilized laser and fiber-based FLFC[37][38]. Those demonstrations revealed that the low-noise local oscillator will confidently replace the CSO as a flywheel of the primary standards in the near future, with removing the use of troublesome cryogenics.

The performance of the FLFCs as the optical-to-optical frequency synthesizer has evaluated by the optical heterodyne comparison of their spectral lines. This method enables to attain the high precision measurement in 10^{-19} range due to the free from the power-to-phase conversion noise caused by the photodiode for the pulse detection[40]. Figure 12(B) shows the configuration for the heterodyne comparison measurement. Both FLFCs are phase locked on the common cavity-stabilized laser. In the optical heterodyne measurement, we can obtain $f_{\text{rep1}} = f_{\text{rep2}}$ by setting $f_{\text{ceo1}} + f_{\text{beat1}} = f_{\text{ceo2}} + f_{\text{beat2}}$. This allows the use of group of lines from each FLFC to generate the strong heterodyne beat signal, since all modes are appropriately synchronized for the signal generation. The SNR of the beat signal was as high as 52 dB with a 300 kHz bandwidth. The fractional instability relative to the reference laser is plotted in Fig. 13(b). The instability starts from 2×10^{-16} at 1 s and averages down to 10^{-18} level in 1000 s. This short-term instability could arise from the Doppler frequency shift of mirror vibrations in the heterodyne interferometer. The estimated level is in agreement with the measurement when the vibration at the Fourier frequency of 1 Hz is assumed to be 10 nm. The relative frequency difference between two FLFCs is equal to 3.4×10^{-18} with an uncertainty of 2.9×10^{-18} within the measurement time of 7700 s. Our FLFCs were found to be available for the frequency measurement of the optical lattice clock with the best performance[39].

4.2 Frequency measurement of 1.5 μm optical communication laser with Er-fiber laser frequency comb

In recent years, optical fiber communications become a very important for the transmission of the information signals. The cw laser oscillating at the 1.5 μm wavelength is one of the key devices for the optical communication and is required to have a narrow linewidth and absolute frequency matched to the ITU grid. We have measured the absolute frequency of a 1.5 μm acetylene-stabilized laser by using NICT-FCF1 and established the frequency measurement procedure. The acetylene-stabilized laser is available for an optical reference in the telecommunication band. It is stabilized to the P(9) rotational line in $\nu_1 + \nu_3$ vibration overtone band of the acetylene isotope $^{13}\text{C}_2\text{H}_2$ at 194 894 844 MHz. The laser output was transmitted through a SM fiber and transferred to an all-fiber heterodyne interferometer for the f_{beat} detection. The f_{beat} signal had a SNR of 29 dB in the RBW of 100 kHz. The f_{beat} spectral linewidth was broadened to be more than 1.5 MHz, which was affected by the frequency jitter noise from the acetylene-stabilized laser. The absolute frequency of the laser was measured over 3 days and is plotted in Fig. 15. The measured frequency was 194 894 844 975 145.2 Hz, which was in accordance with the la-

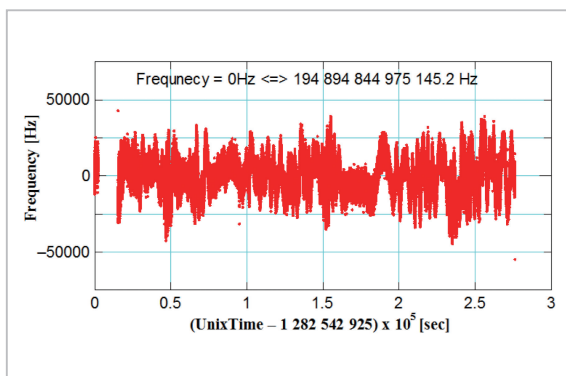


Fig.15 Absolute frequency measurements of the acetylene-stabilized 1.5 μm light source

Absolute frequency measurement of Acetylene stabilized laser by fiber laser frequency comb over a period of 3 days. The frequency offset of 194 894 844 975 145.2 Hz is subtracted from the absolute frequency.

ser specification. Figure 16(a) shows the Allan standard deviation of the acetylene-stabilized laser. The frequency instability was measured to be below 3×10^{-11} . From this measurement, the NICT-FCF1 was found to be applied for the performance evaluation of the 1.5 μm laser for optical-fiber communications. It is also suited for the future optical clocks requiring the stable continuous operation of over days.

We have also measured a cavity-stabilized 1.5 μm DFB fiber laser to determine the measurement precision of the NICT-FCF1. The NICT-FCF1 was referenced to the CSO with the fractional stability of 10^{-16} level as shown in Fig. 16(c). Figure 16(d) shows the instability of the DFB laser against the CSO via the NICT-FCF1. From the result, the measurement precision of the NICT-FCF1 was reached at least 3×10^{-14} in 1 s. The frequency drift due to the length variation of the reference cavity for the DFB laser was appeared over the 3 s averaging times. Further verification of the measurement precision of the NICT-FCF1 is expected by the comparison of two independent fiber-based FLFC referenced to common microwave or optical reference.

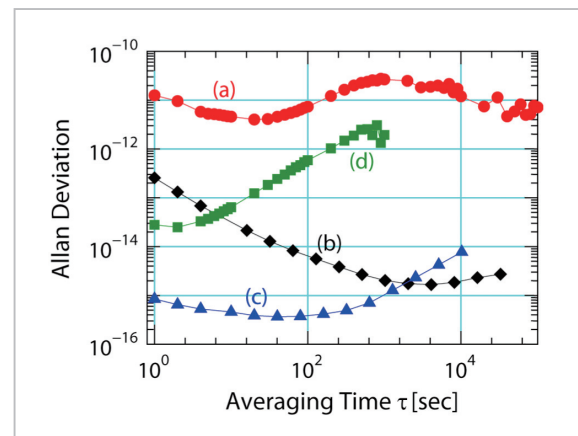


Fig.16 Frequency stability of the 1.5 μm light source measured with fiber optical frequency comb

Measured frequency instabilities as given by the Allan standard deviation. (a) Acetylene stabilized laser vs H-maser. (b) Instability of H-maser employed as rf-reference. (c) Instability of cryogenic sapphire oscillator (CSO) [41]. (d) DFB fiber laser vs CSO via fiber comb.

5 Conclusion and outlooks

A self-referenced optical frequency comb generated from a fs-pulse mode-locked laser enables direct connection of separate optical frequencies and link optical to microwave frequency with high precision. Such FLFCs have many scientific and technological applications, including metrology, atom and molecular spectroscopy, astronomy and high-energy physics. In this article, we presented the characteristics of the FLFCs developed. They have been actually applied to determine the clock transition frequency of $^{40}\text{Ca}^+$ ions^[42] and ^{87}Sr atoms^[43] with the uncertainty of 10^{-15} level. From these measurements, the FLFCs were found to be suitable for the optical frequency standards. The achieved performance of our FLFCs was a significant milestone for the establishment of the optical standards in NICT and contribution to the re-definition of SI second.

The optical comb generation from various type of lasers and possible extensions of their wavelength coverage are very interesting topics, although they have not been reported in this article. Although the potential for using mode-locked lasers in optical comb generation was recognized early, these lasers did not provide the properties necessary for fulfilling this potential. The development of the Kerr-lens mode-locked Ti:sapphire laser has been largely contributed to the first frequency measurement based on FLFC. It had capability to generate ultra-short pulses so that the spectral broadening exceeding an optical octave was finally succeeded by using external nonlinear devices. Currently the fastest f_{rep} was reached as high as

10 GHz^[44]. Such high f_{rep} is especially suitable for the astronomical application due to the convenience for the mode number determination. Thereafter, the development of optical comb based on rare-earth-doped fiber mode-locked lasers was attractive because of their advantages: size, cost, transportability, maintenance-free and long-term operational stability. The generation of optical combs in a monolithic ultra-high-Q microresonator was recently reported as a different approach, in which equally spaced frequency markers were produced by interaction between a cw pump laser with the modes of the silica toroidal microresonator via the Kerr nonlinearity. This intrinsically simple system might be available such for space based optical clocks along with the technology of space optical communications. Considering the importance of optical comb in various fields, the semiconductor laser directly generating the optical comb is anticipated in terms of downsizing, weight saving, and cost reduction. Meanwhile, the spectral extension of FLFC is crucial to fully benefit from their potential. It was started in the visible and near-infrared regions by using the Ti:sapphire lasers and rare-earth-doped fiber lasers. High-harmonic generation has employed to move toward shorter wavelength over the ultra-violet region^[47]^[48], while parametric down conversion processes including the difference frequency generation were used to cover the mid-infrared region^[49]. For the needs of various scientific fields, it is also supposed to keep covering the wavelength regions that have not been illuminated by the existing FLFCs.

References

- 1 H. Mabuchi, J. Ye, and H.J. Kimble, *Appl. Phys. B: Lasers Opt.*, Vol. B68, pp. 1095–1108, 1999.
- 2 V.A. Dzuba and V.V. Flambaum, *Phys. Rev. A*, Vol. 61, 034502, 2000.
- 3 S.G. Karshenboim and E. Peik, *Astrophysics, Clocks and Fundamental Constants* (Springer, Berlin, 2004).
- 4 H. Schnatz, B. Lipphardt, J. Helmcke, F. Riehle, and G. Zinner, *Phys. Rev. Lett.*, Vol. 76, pp. 18–21, 1996.

- 5 D.J. Jones, S.A. Diddams, J.K. Ranka, A. Stentz, R.S. Windeler, J.L. Hall, and S.T. Cundiff, *Science*, Vol. 288, pp. 635–639, 2000.
- 6 R. Holzwarth, T. Udem, T.W. Hansch, J.C. Knight, W.J. Wadsworth, and P.St.J. Russell, *Phys. Rev. Lett.*, Vol. 85, pp. 2264–2267, 2000.
- 7 S.T. Cundiff, J. Ye, and J.L. Hall, *Rev. Sci. Instrum.*, Vol. 72, pp. 3749–3771, 2001.
- 8 J.C. Knight, *Nature*, Vol. 424, pp. 847–851, 2003.
- 9 L. Hollberg, C.W. Oates, E.A. Curtis, E.N. Ivanov, S.A. Diddams, Th. Udem, H.G. Robinson, J.C. Bergquist, R.J. Rafac, W.M. Itano, R.E. Drullinger, and D.J. Wineland, *IEEE J. Quantum Electron.*, Vol. 37, pp. 1502–1513, 2001.
- 10 R. Ell, U. Morgner, F.X. Kartner, J.G. Fujimoto, E.P. Ippen, V. Scheuer, G. Angelow, and T. Tschudi, *Opt. Lett.*, Vol. 26, pp. 373–375, 2001.
- 11 R. Szipocs, K. Ferencz, C. Spielmann, and F. Krausz, *Opt. Lett.*, Vol. 19, pp. 201–203, 1994.
- 12 H. Inaba, Y. Daimon, F.-L. Hong, A. Onae, Ka. Minoshima, T.R. Schibli, H. Matsumoto, M. Hirano, T. Okuno, M. Onishi, and M. Nakazawa, *Opt. Express*, Vol. 14, pp. 5223–5231, 2006.
- 13 W.C. Swann, J.J. McFerran, I. Coddington, N.R. Newbury, I. Hartl, M.E. Fermann, P.S. Westbrook, J.W. Nicholson, K.S. Feder, C. Langrock, and M.M. Fejer, *Opt. Lett.*, Vol. 31, pp. 3046–3048, 2006.
- 14 J.J. McFerran, W.C. Swann, B.R. Washburn, and N.R. Newbury, *Appl. Phys. B*, Vol. 86, pp. 219–227, 2007.
- 15 H. Ito, S. Nagano, and M. Hosokawa, *Jpn. J. Opt.*, Vol. 36, pp. 85–87, 2007.
- 16 http://www.bipm.org/jst/en/kcdb_data.jsp
- 17 O. Mucke, R. Ell, A. Winter, J. Kim, J. Birge, L. Matos, and F. Kartner, *Opt. Express*, Vol. 13, pp. 5163–5169, 2005.
- 18 M. Prevedelli, T. Freearde, and T.W. Hansch, *Appl. Phys.*, Vol. B60, pp. S241–S248, 1995.
- 19 J. Reichert, R. Holzwarth, Th. Udem, and T.W. Hansch, *Opt. Commun.*, Vol. 172, pp. 59–68, 1999.
- 20 F.L. Walls and A. De Marchi, *IEEE Trans. Instrum. Meas.*, Vol. 24, pp. 210–217, 1975.
- 21 A. Bartels and H. Kurz, *Opt. Lett.*, Vol. 27, pp. 1839–1841, 2002.
- 22 T.M. Ramond, S.A. Diddams, L. Hollberg, and A. Bartels, *Opt. Lett.*, Vol. 27, pp. 1842–1844, 2002.
- 23 M. Nakazawa, E. Yoshida, T. Sugawa, and Y. Kimura, *Electronics Letters*, Vol. 29, pp. 1327–1329, 1993.
- 24 G.P. Agrawal, *Nonlinear Fiber Optics*, Second Edition, Academic Press, New York, 1995.
- 25 S.M.J. Kelly, *Electron. Lett.*, Vol. 30, pp. 806–808, 1992.
- 26 F. Adler, K. Moutzouris, A. Leitenstorfer, H. Schnatz, B. Lipphardt, and G. Grosche, *Opt. Exp.*, Vol. 12, pp. 5872–5880, 2004.
- 27 S. Nagano, H. Ito, Y. Li, K. Matsubara, and M. Hosokawa, *Jpn. J. Appl. Phys.*, Vol. 48, 042301, 2009.
- 28 Y. Li, S. Nagano, K. Matsubara, H. Ito, M. Kajita, and M. Hosokawa, *Jpn. J. Appl. Phys.*, Vol. 47, pp. 6327–6332, 2008.
- 29 A. Bartels, C.W. Oates, L. Hollberg, and S.A. Diddams, *Opt. Lett.*, Vol. 29, pp. 1081–1083, 2004.
- 30 J. Ye, J.L. Hall, and S.A. Diddams, *Opt. Lett.*, Vol. 25, pp. 1675–1677, 2000.
- 31 E.N. Ivanov, S.A. Diddams, and L. Hollberg, *IEEE J. Sel. Top. Quantum Electron.*, Vol. 9, pp. 1059–1065, 2003.
- 32 A. Bartels, S.A. Diddams, T.M. Ramond, and L. Hollberg, *Opt. Lett.*, Vol. 28, pp. 663–665, 2003.
- 33 C. Vian, P. Rosenbusch, H. Marion, S. Bize, L. Cacciapuoti, S. Zhang, M. Abgrall, D. Chambon, I. Maksimovic, P. Laurent, G. Santarelli, A. Clairon, A. Luiten, M. Tobar, and C. Salomon, *IEEE Trans. Instrum. Meas.*, Vol. 54, pp. 833–836, 2005.

-
- 34 G.J. Dick, J.D. Prestage, C.A. Greenhall, and L. Maleki, Proceedings of the 22nd Annual Precise Time and Time Interval (PTTI), pp. 487–508, 1990.
 - 35 K. Watabe, H. Inaba, K. Okumura, F.-L. Hong, J.G. Hartnett, C.R. Locke, G. Santarelli, S. Yanagimachi, K. Minoshima, T. Ikegami, A. Onae, S. Ohshima, and H. Matsumoto, IEEE Trans.Instrum.Meas., Vol. 56, pp. 632–636, 2007 .
 - 36 S. Chang, A.G. Mann, and A.N. Luiten, Electron. Lett., Vol. 36, pp. 480–481, 2000.
 - 37 J. Millo, M. Abgrall, M. Lours, E.M.L. English, H. Jiang, J. Guena, A. Clairon, M.E. Tobar, S. Bize, Y. Le Coq, and G. Santarelli, Appl. Phys. Lett., Vol. 94, 141105, 2009.
 - 38 B. Lipphardt, G. Grosche, U. Sterr, C. Tamm, S. Weyers, and H. Schnatz, IEEE Trans. Instrum. Meas., Vol. 58, pp. 1258–1262, 2009.
 - 39 A.D. Ludlow, T. Zelevinsky, G.K. Campbell, S. Blatt, M.M. Boyd, M.H.G. de Miranda, M.J. Martin, J.W. Thomsen, S.M. Foreman, Jun Ye, T.M. Fortier, J.E. Stalnaker, S.A. Diddams, Y. Le Coq, Z.W. Barber, N. Poli, N.D. Lemke, K.M. Beck, and C.W. Oates, Science, Vol. 319, pp. 1805–1808, 2008.
 - 40 L.S. Ma, Z. Bi, A. Bartels, L. Robertsson, M. Zucco, R.S. Windeler, G. Wilpers, C.W. Oates, L. Hollberg, and S.A. Diddams, Science, Vol. 303, pp. 1843–1845, 2004.
 - 41 J.G. Hartnett, C.R. Locke, E.N. Ivanov, M.E. Tobar, and P.L. Stanwix, Appl. Phys. Lett., Vol. 89, 203513, 2006.
 - 42 K. Matsubara, K. Hayasaka, Y. Li, H. Ito, S. Nagano, M. Kajita, and M. Hosokawa, Appl. Phys. Express, Vol. 1, 067011, 2008.
 - 43 A. Yamaguchi, N. Shiga, S. Nagano, H. Ishijima, Y. Koyama, M. Hosokawa, and T. Ido, “A Strontium Optical Lattice Clock,” Special issue of this NICT Journal, 3-3, 2010.
 - 44 A. Bartels, D. Heinecke, and S.A. Diddams, Science, Vol. 326, p. 681, 2009.
 - 45 T.R. Schibli, I. Hartl, D.C. Yost, M.J. Martin, A. Marcinkewius, M.E. Fermann, and J. Ye, Nature Photonics, Vol. 2, pp. 335–339, 2008.
 - 46 P. Del’Haye, T. Herr, E. Gavartin, R. Holzwarth, and T.J. Kippenberg, arXiv:0912.4890v1, 2009.
 - 47 R.J. Jones, K.D. Moll, M.J. Thorpe, and J. Ye, Phys. Rev. Lett., Vol. 94, 193201, 2005.
 - 48 S. Kim, J. Jin, Y.J. Kim, I.Y. Park, Y. Kim, and S.W. Kim, Nature, Vol. 453, pp. 757–760, 2008.
 - 49 T. Yasui, Y. Kabetani, E. Saneyoshi, S. Yokoyama, and T. Araki, Appl. Phys. Lett., Vol. 88, 241104, 2006.

(Accepted Oct. 28, 2010)

NAGANO Shigeo, Ph.D.

Senior Researcher, Space-Time Standards Group, New Generation Network Research Center

Optical Frequency Standards, Space-Time Measurements

ITO Hiroyuki, Ph.D.

Senior Researcher, Space-Time Standards Group, New Generation Network Research Center

Atomic Frequency Standard, Optical Frequency Standards



LI Ying, Ph.D.

Senior Researcher, Space-Time Standards Group, New Generation Network Research Center

Optical Frequency Standards, Laser Physics



KUMAGAI Motohiro, Ph.D.

Senior Researcher, Space-Time Standards Group, New Generation Network Research Center

Atomic Frequency Standard, Frequency Transfer using Optical Fibers



Clayton R. Locke, Ph.D.

Invited Executive Researcher, Space-Time Standards Group, New Generation Network Research Center

Optical Frequency Standards, Space-Time Measurements

John G. Hartnett, Ph.D.

Professor, School of Physics, University of Western Australia

Microwave Frequency Standards, Space Time Measurement



HOSOKAWA Mizuhiko, Ph.D.

Executive Director, New Generation Network Research Center

Atomic Frequency Standards, Space-Time Measurements